This article has been accepted for publication in a future issue of this journal, but has not been fully edited. Content may change prior to final publication. Citation information: DOI 10.1109/TAP.2014.2334358, IEEE Transactions on Antennas and Propagation

Simply-Fed Four-Arm Spiral-Helix Antenna

Mohamed A. Elmansouri, James B. Bargeron, and Dejan S. Filipovic

***Abstract*— An ultra-wideband four-arm spiral-helix antenna with simple beamformer is developed to have simultaneously good performance in time and frequency. Two microstrip feeds printed on the opposite side of the spiral with impedance following Klopfenstein taper are employed to eliminate the need for 180° hybrids used in conventional beamformers. Ferrite beads placed around the coaxial cables connected between the ground and microstrip are utilized to choke unbalanced currents and prevent shorting the spiral aperture to the ground. Helix is used to improve the low-frequency performance and allow easy attachment of resistive loading to the ground plane. A metallic inset is placed inside the cavity to eliminate the destructive pattern interference and improve the high-frequency gain. To achieve low dispersion, the spiral is loosely wrapped. Simultaneously good time and frequency domain performance from 0.5GHz to 3GHz with VSWR<2, nominal gain and radiation efficiency of 6dBic and 80%, respectively, broadside axial ratio below 1.8dB and fidelity factor of 93% over wide field of view are demonstrated in simulations and experiments.**

***Index Terms*— Fidelity factor, four-arm spiral antenna, spiral-helix antenna, time-domain.**

I. Introduction

Four-arm spiral antennas are known for multi-mode capability and superior frequency-domain performance compared to their two-arm spiral counterparts [1]. The detailed modal analysis in [2] showed that the multiple arms act as modal filter that eliminates the radiation of undesired modes, thus enabling the four-arm spiral to achieve very low axial ratio and high pattern purity over wide bandwidth and field of view. In addition, loosely wrapped four-arm spirals may achieve simultaneously good frequency-domain radiation and very low-dispersion [3] thus extending their candidacy for applications needing antennas with simultaneously good time and frequency responses. However, two issues remain, specifically, the efficiency and the complexity of the feed network. Both shortcomings are overcome in this work. Experiments and simulations are used to verify the improvements in frequency- and time-domain responses compared to the more conventional designs.

To achieve unidirectional and consistent patterns with planar spirals they are typically backed by an absorber. This reduces antenna's gain for 3dB or more with nominal total efficiency falling under 50%. The use of metallic backing with a conventional spiral without any treatment of arms [4]-[6] or cavity [6]-[8] deteriorates significantly the impedance match and the far-field performance when multiple octave bandwidths are desired for their use.

A viable approach to maintain good frequency-domain performance with a metallic backing is to terminate the spiral's arms with quadrifilar helix having attached lumped resistors at its bottom end. This approach is discussed in [9] wherein the benefits of using the helix termination to improve the four-arm spiral's low-end gain and eliminate circular cavity modes are demonstrated. To make the four-arm spiral-helix antenna more practical, the complexity of the beamformer needs to be reduced. In this paper, the main objective is to reduce the complexity of antenna's beamformer and thus allow for a four-arm spiral antenna to be a serious contender to the more established two-arm configuration for many commercial and defense applications. Specifically, a combined embedded coaxial / planar tapered dual-microstrip feeding arrangement is proposed to mitigate the issues associated with the mode 1 beamforming of a four-arm spiral-helix antenna while maintaining good time-domain and frequency-domain performances over at least 6:1 bandwidth. Microstrip feed is designed to perform impedance transformation and 180° phase offset between the sets of opposite arms in a similar way as shown with a two-arm spiral from [10]. This way, the need for the 2nd row of the modified Butler matrix beamformer [1]-[2] composed of two 180° hybrids is eliminated. The microstrip ground at the taper's outside end is used to solder the shield of a coaxial cable which routes the signal under the antenna ground plane into a 90° hybrid needed to establish the required mode 1 phasing. To prevent shorting of the aperture to the ground, a row of ferrite beads wrapped around coaxial cables is placed between the coax-to-microstrip transition and cavity bottom. Over the considered 0.5-3GHz bandwidth, the fabricated antenna has measured fidelity factor >90%, VSWR <2, axial ratio < 1.8dB, high efficiency, and consistent patterns with nominal gain of 6dBic. Good agreement with theory verifies the quality of prototyping and soundness of the proposed design principles.

II. Antenna Description

A conventional beamformer for a mode 1 four-arm spiral has two 180° and one 90° hybrid as shown in Fig. 1(a). While a decade bandwidth components are available, they are expensive, bulky, and lossy with higher imbalances that negatively impact the antenna performance. In addition, the internal port of 180° hybrid must be terminated which altogether brings forth the need for a beamformer housing further increasing the cost, design and platform integration challenges. To reduce the complexity of the feed network, a planar microstrip feed is developed as shown in Fig. 1(b). The designed microstrip feed has a spiral shape and it is based on Klopfenstein impedance taper [10] that transforms 50Ω impedance at the input of the coaxial feed to 140Ω at the center of the spiral. The metallic spiral arms act as a ground plane for the two microstrip lines. The above described planar microstrip impedance transformers are used to feed the two sets of opposite arms of the antenna thus achieving the required 180°

Manuscript received March 11, 2014. This work is sponsored by the Office of Naval Research (ONR) award #N00014-10-C-0467.

M. Elmansouri, J. Bargeron, and D. S. Filipovic are with the Department of Electrical, Computer, and Energy Engineering, University of Colorado, Boulder, CO 80309-0425 USA (e-mail: dejan.filipovic@colorado.edu).

This article has been accepted for publication in a future issue of this journal, but has not been fully edited. Content may change prior to final publication. Citation information: DOI 10.1109/TAP.2014.2334358, IEEE Transactions on Antennas and Propagation

phase difference and eliminating the need for the hybrids in Fig. 1(a).

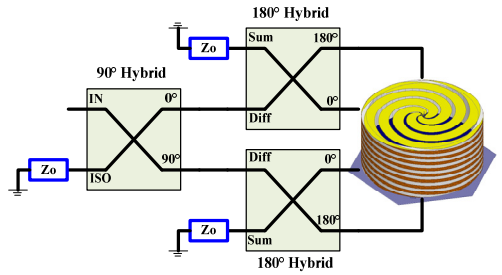

(a)

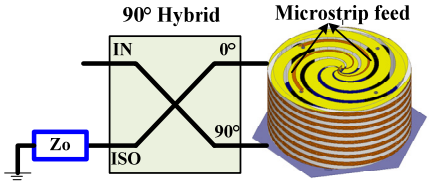

(b)

Fig.1. (a) Conventional way to excite mode 1 operation of a four-arm spiral-helix antenna, and (b) proposed microstrip feeding technique to reduce the beamformer complexity.

The typical issues with this feeding scheme include the asymmetry in the feeding structure, radiation from the feed, fringing fields especially with a narrow ground plane, and coupling between the microstrip and the spiral's traveling-wave currents. These may degrade the far-field performance so their impact needs to be evaluated. To reduce the coupling between the microstrip and spiral travelling waves the width of the microstrip signal line should be as small as possible (compared to the width of the spiral arm). To do so, different methods may be considered including, reducing the number of turns (i.e. increasing the growth rate), increasing the spiral's metal to slot ratio (MSR), reducing the substrate thickness or increasing its permittivity. If the growth rate, MSR, and the substrate permittivity/height are too high, the spiral's performance will be deteriorated even with an ideal feed [2]. Here we choose Archimedean spiral since it has a constant arm width which lands itself nicely with the proposed feeding scheme. A single-turn (N=1) spiral is adopted not only to realize the aforementioned criteria but also to maintain low-dispersion and pulse distortion [3].

The effect of the MSR is studied first. A spiral aperture with outer radius of r_{out} =7.6cm and inner radius of r_{in} = 0.2cm is modeled on a 0.508mm thick Rogers RO3003 substrate ($\varepsilon_r = 3, \tan\delta = 0.0013$) in ANSYS HFSS with different MSRs. Increasing the MSR reduces the spiral's input impedance which, as shown in Fig. 2, allows better impedance match while maintaining realizable feed's dimensions with the chosen substrate height (H). The VSWR noticeably improves as MSR increases from 1:1 (self complementary) to 5:1 while the gain is only slightly affected. The axial ratio and the consistency of the far-field patterns are also not significantly impacted by the increased MSR. Thus, to achieve good impedance match and far-field performance, the single-turn Archimedean four-arm spiral with 5:1 MSR is selected.

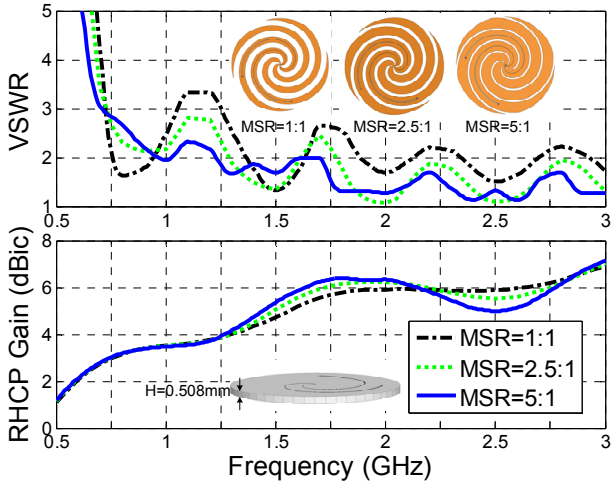

Fig.2. Effects of the metal-to-slot-ratio (MSR) on the VSWR and broadside co-polarized gain of microstrip-fed spiral antenna.

A 0.508 thick RO3003 substrate is used instead of thicker substrates since the numerical studies demonstrated that better radiation patterns and performance similar to the ideally-fed spiral can be achieved with thinner substrates (see Fig. 3). As seen, the lower VSWR and enhanced far-field characteristics (only axial ratio at θ=30° off boresight is shown here, but the same observations are seen for other parameters) are obtained with 0.508mm substrate. Also, similar performance to ideal feed (modeled as two lumped ports in HFSS) is observed indicating negligible radiation interference from the microstrip feed. Minimum and maximum microstrip feed widths are 0.13mm and 1.28mm respectively. Minimum microstrip to ground plane width ratio of 1:11.7 is obtained with this design.

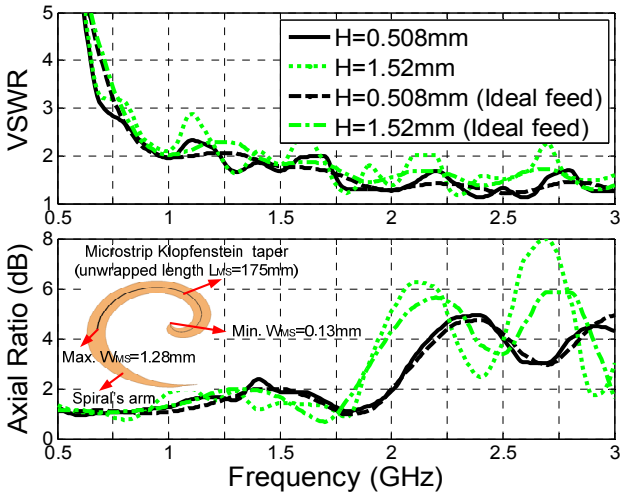

Fig.3. Effects of the substrate height (H) on the VSWR and axial ratio at θ=30° of microstrip-fed spiral antenna (MSR=5:1). Dimensions of the microstrip impedance taper for 0.508mm thick substrate are also shown in the inset.

Another critical design aspect which significantly affects the antenna's impedance match is the transition region between the microstrip line and the spiral arms. Zoomed model of this transition region along with the greater engineering details for the entire feed realization are shown in Fig. 4. Since the nominal mode 1 impedance for this transition is twice the impedance to the ground (of mode 1), the elaborate full-wave

This article has been accepted for publication in a future issue of this journal, but has not been fully edited. Content may change prior to final publication. Citation information: DOI 10.1109/TAP.2014.2334358, IEEE Transactions on Antennas and Propagation

study is carried out to achieve an acceptable return loss. Circular pads are added to the feed lines to better support the fabrication of plated vias used to directly connect the microstrip's signal line and the spiral arms. Notice that the pads only slightly affect the antenna performance.

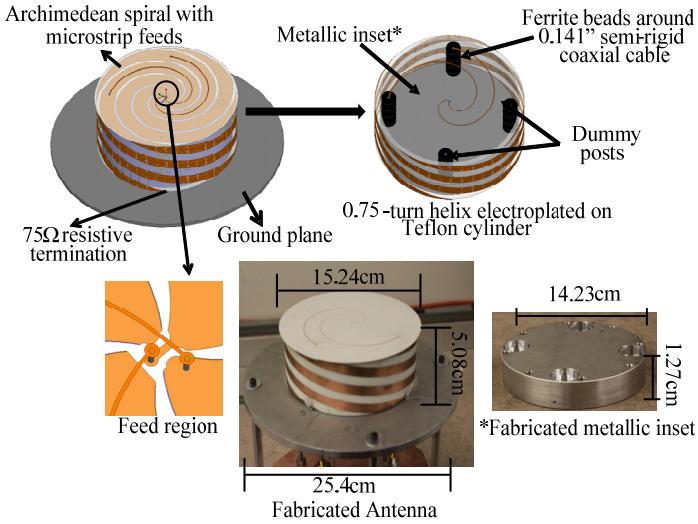

Fig.4. Configuration details of the developed spiral-helix antenna.

The self-complementary quadrifilar helix has 0.75-turns and height of 5.08cm and it is electroplated on a hollow Teflon cylinder as discussed in [9]. The helix parameters are derived from different parametric studies with a chief goal of achieving highest gain at the low-end while maintaining overall good performance over the designated bandwidth. The helix top ends are carefully soldered to the spiral arms. In order to provide an acceptable impedance match over the frequency range of operation, the lumped resistive loading is implemented between the bottom arm ends of the quadrifilar helix and the ground plane. Full-wave simulations have shown that the 75Ω resistors (one resistor per arm) provide the best compromise between the impedance match and efficiency.

The destructive pattern interference that occurs at 3GHz for a 5.08cm (~λ/2) cavity [11] is mitigated by inserting a 1.27cm tall, 14.23cm diameter metal cylinder inside the cavity. This inset pushes the frequency of the destructive pattern interference beyond 3GHz while only slightly affecting the lower-band performance as clearly demonstrated in Fig. 5 where the co-polarized gain (i.e. RHCP gain) of the proposed spiral-helix is plotted in the cases with and without (w/o) inset. Although the VSWR performance of the antenna without the inset is still below 2 (not shown here), the deterioration of gain and axial ratio as seen in Fig. 5 limits the highest frequency of operation to 2.25GHz. To choke the currents on the outer conductor of the coaxial feed cables that may short the spiral and the helix to the ground plane, ferrite beads (LairdTech. HFB 15203) are placed around the coaxial cable feeds and corresponding dummy posts used for symmetry. A single 90° hybrid (Werlatone QH7902) is used to feed the antenna as shown in Fig. 1(b). A fully assembled spiral-helix is placed on a 25.4cm diameter circular ground plane. The relevant details of the final antenna structure are shown in Fig. 4.

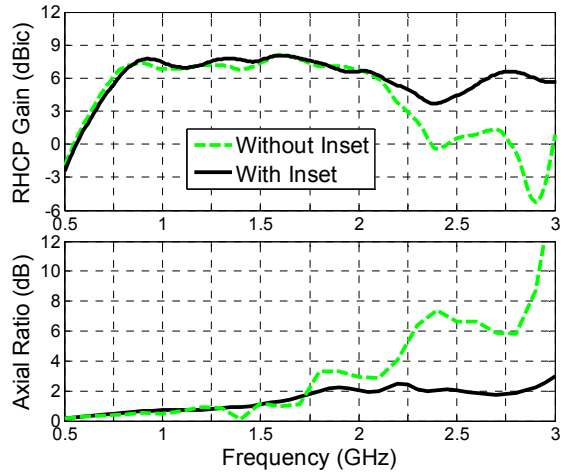

Fig.5. Simulated co-pol. gain and axial ratio at θ=30°of the designed spiral-helix antenna with and without the cylindrical inset.

III. Frequency-Domain Performance

Measured and simulated active VSWRs at the port 1 of the proposed antenna, shown in Fig. 4, are shown in Fig. 6. As seen, VSWR less than 2 is measured from 0.5 GHz to 3 GHz indicating a very good performance of the proposed feeding approach. The coupling between the antenna's ports is below -35dB whereas the other port has similar VSWR as that shown in Fig. 6. To demonstrate the impact of ferrite beads, the simulated VSWR of the antenna without the ferrite beads is also plotted. As seen, the match is significantly deteriorated at the low-end due to shorting the spiral aperture to the ground. Effectively, the helix contribution to the total radiated field and low-frequency impedance match is negated if the beads are not used.

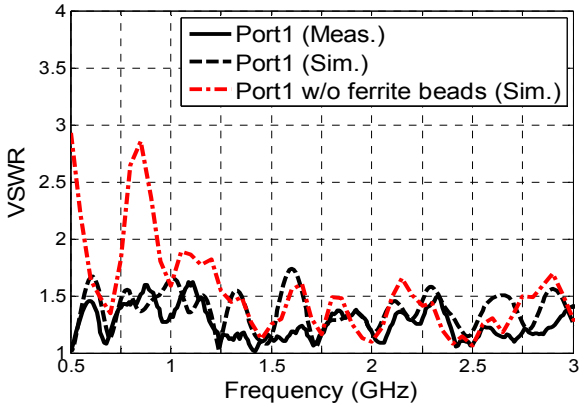

Fig.6. Measured and simulated active VSWRs at the port 1 of the spiral-helix antenna (shown in Fig. 4) with and without ferrite beads.

Measured normalized co-polarized (RHCP) and cross-polarized (LHCP) radiation patterns of the antenna at different frequencies overlaid over 61 azimuthal cuts from 0° to 180° are shown in Fig. 7. While not commonly used in open literature, this far-field representation is helpful to visually assess the consistency of the radiation patterns of wideband antennas. As seen, consistent and symmetric mode 1 patterns are obtained over the operating bandwidth. Azimuthal gain variation less than 2dB is measured up to the elevation angle θ=30° further demonstrating high quality radiation patterns. Front to back ratio better than 30dB is also measured.

This article has been accepted for publication in a future issue of this journal, but has not been fully edited. Content may change prior to final publication. Citation information: DOI 10.1109/TAP.2014.2334358, IEEE Transactions on Antennas and Propagation

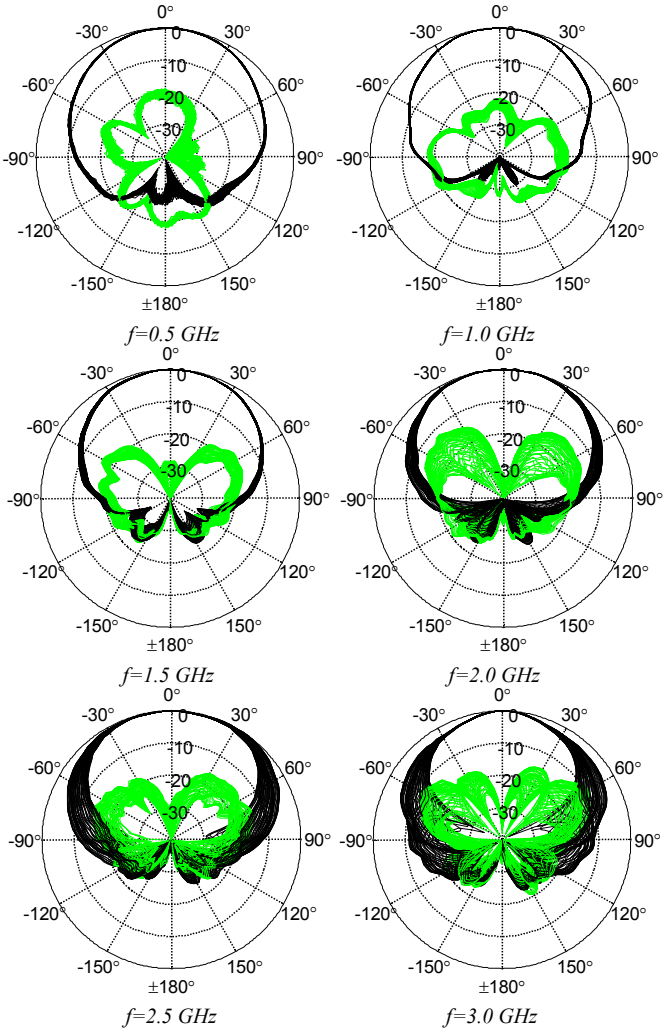

Fig.7. Measured overlaid radiation patterns of the spiral-helix antenna for 61 azimuthal cuts from 0° to 180° (dark: RHCP, light: LHCP).

The low cross-polarization level at the broadside seen in Fig. 7 is more explicitly observed in Fig. 8 where the ratio is plotted. As seen, values below 1.8 dB are measured over the operating bandwidth. Moreover, the axial ratio below 3dB up to the elevation angle of θ=30° off broadside is obtained. A slight degradation at the low-end is due to the range imperfections. The obtained high quality radiation patterns and low axial ratio clearly demonstrate that the microstrip feed and the entire antenna construction including its structural parameters have minimal negative impact. Moreover, due to the feed symmetry, the impact of 180° hybrid imbalances in Fig. 1(a), is completely eliminated.

Measured and simulated realized gain and radiation effeciency are shown in Fig. 9. As seen, the realized gain is above 5dBic over the majority of operating bandwidth (nominal 6dBic) with 0dBic measured at 530MHz. The importance of the ferrite beads is also demonstrated in Fig. 9. When compared to the case without the beads, notice the gain improvement of up to 6dB through 0.9GHz. The gain slightly reduces at higher frequencies due to losses in the ferrite. The radiation effeicency is greater than 50% starting from 730MHz and reaches maximum of 92% at the mid-band around 1.5GHz. Its nominal value is ~80%. A reduced efficiency at the low-end is due to the power loss in the resisitve termination. The proposed spiral-helix shows similar and even better performance compared to the center-fed spiral-helix antenna in [9]. Notice that the operational bandwidth of the proposed antenna is limited by the used 90° hybrid. The full-wave modeling showed that this antenna can operate with good radiation characteristics over almost 10:1 bandwidth. Throughout this section a good agreement between the measurements and HFSS-simulations is obtained.

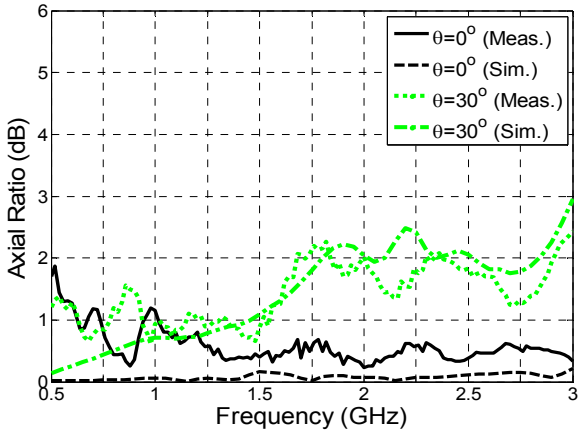

Fig.8. Measured and simulated axial ratio of the spiral-helix antenna at boresight and θ=30°.

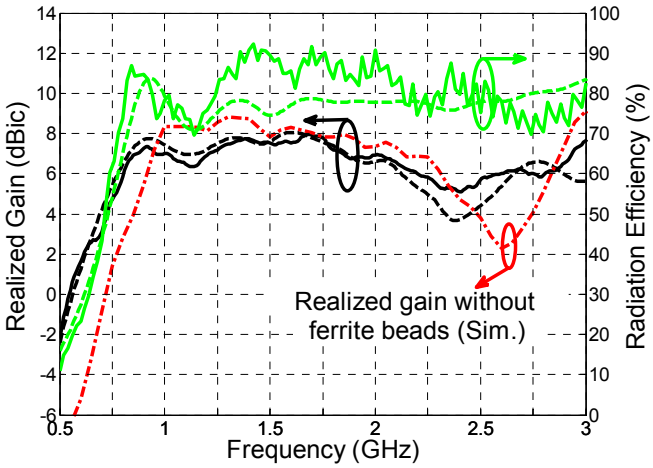

Fig.9. Measured (solid) and simulated (dashed) co-pol. realized gain (RHCP), and radiation efficiency. The realized gain without ferrite beads is also shown.

IV. Time-Domain Performance

To characterize the time-domain performance of the fabricated antenna, its transfer function is determined first. The link's transfer function (S_{21}) of two nearly identical spiral-helix antennas is measured in anechoic chamber using the vector network analyzer Agilent PNA-x 5245A. After obtaining the antenna transfer function at the boresight ($\theta = 0^o, \varphi = 0^0$) following the procedures in [12], one antenna which will be considered as reference antenna is kept fixed while the antenna under test (AUT) is rotated in azimuthal and elevation planes with $\Delta\theta = \Delta\varphi = 3^o$ in order to characterize the time-domain performance over the full-field of view. Measurements are conducted from 0.3 GHz to 4 GHz with 10 MHz resolution. Then, the measured link's transfer

This article has been accepted for publication in a future issue of this journal, but has not been fully edited. Content may change prior to final publication. Citation information: DOI 10.1109/TAP.2014.2334358, IEEE Transactions on Antennas and Propagation

function is used to evaluate the transmitting antenna transfer function (i.e. radiation transfer function) [13].

The measured and simulated group delays derived from the phase response of the transfer function at boresight along xz-plane are shown in Fig. 10. As seen, low group delay variation is obtained indicating good dispersion characteristics which is expected since the spiral has only a single turn. The measured radiated pulses of the antenna, obtained from the measured transfer function and inverse fast Fourier transform (IFFT) at different elevation angles are shown in the inset of Fig. 11. The simulated radiated pulses obtained from direct time-domain analysis in CST Microwave Studio are also included. As seen, high quality pulse radiation is obtained over the wide elevation angles. The used source pulse waveform is the second derivative Gaussian pulse ($\sigma = 145\ ps$) [14] (see the inset of Fig. 11) with the 10 dB power spectral density (PSD) bandwidth from 0.40 GHz to 3.2 GHz.

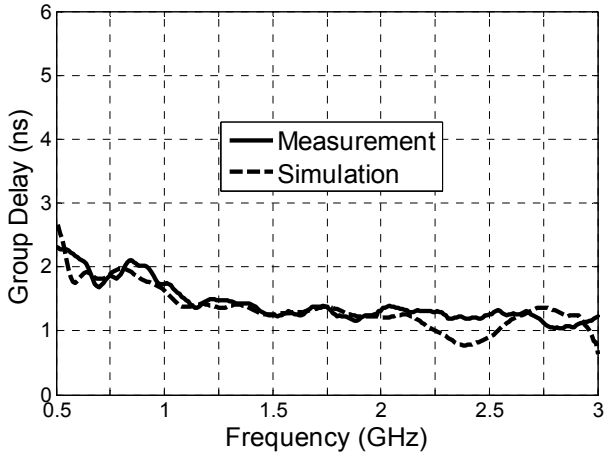

Fig.10. Measured and simulated group delay of the spiral-helix antenna at the boresight along xz-plane.

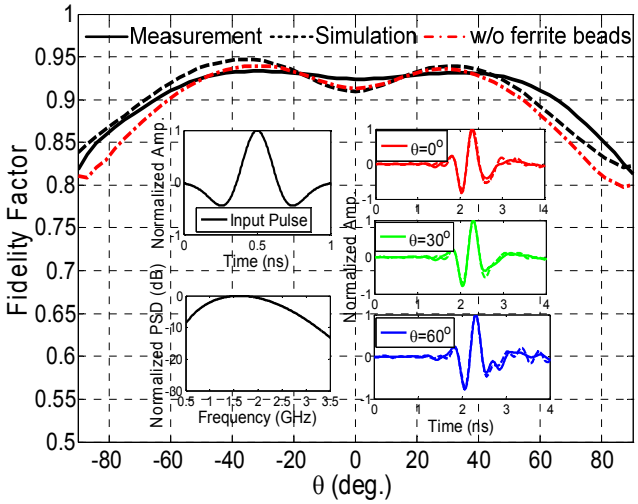

Fig.11. Measured and simulated (with and without ferrite) fidelity factors averaged over 61 azimuthal cuts. Inset: Measured (solid) and simulated (dashed) radiated pulses at different elevation angles xz-plane.

To characterize the quality of the radiated pulses, fidelity factor, which represents the maximum cross correlation between input and radiated pulses obtained for varying time delay, is used [3],[13]. Measured and simulated fidelity factors averaged over 61 azimuthal cuts from 0° to 180° are shown in Fig. 11. The fidelity factor > 90% with the maximal azimuthal variation of about 8% is further proof of antenna's excellent time-domain response. The highest and lowest fidelity factors measured at broadside when the antenna rotates in the φ-plane are 0.95 and 0.88, respectively. The used ferrite chokes have slight effect in time-domain since they are only affecting the transfer function magnitude response (i.e. realized gain) at the low-end where the source pulse has low PSD.

V. Conclusion

A spiral-helix antenna with excellent time- and frequency-domain performances and simple feeding scheme is presented. The proposed combined embedded coaxial / planar tapered dual-microstrip feeding arrangement allows a simple beamformer realization while preserving excellent radiation characteristics. In doing so, it is seen that the ferrite chokes are critically important for the proposed feed scheme to work over the entire bandwidth. VSWR < 2, broadside axial ratio < 1.8dB, radiation efficiency > 80% over most of the bandwidth, consistent patterns and fidelity factor > 90% over wide field of view are obtained experimentally and in simulations. The realized low-profile and low-cost spiral-helix antenna is a viable candidate for different frequency- and time-domain applications including communications and electronic warfare.

References

[1] R. G. Corzine and J. A. Mosko*, Four-Arm Spiral Antennas*. Norwood, MA: Artech House, 1990.

[2] D. S. Filipovic and T. P. Cencich Sr.,"Frequency independent antennas," in *Antenna Engineering Handbook*, 4th ed. New York: Mc-Graw Hill, 2007, ch. 13.

[3] M. A. Elmansouri and D. S. Filipovic, "Pulse distortion and mitigation thereof in spiral antenna-based UWB communication systems," *IEEE Trans. Antennas Propag.*, vol.59, no.10, pp.3863-3871, Oct. 2011.

[4] M. Buck and D. S. Filipovic, "Spiral cavity backing effects on pattern symmetry and modal contamination," *IEEE Antennas and Wireless Propag. Lett.,* vol. 5, pp. 243–247, 2006.

[5] J. L. Volakis, M. W. Nurnberger, and D. S. Filipović, "A broadband cavity–backed slot spiral antenna" *IEEE Antennas Propagat. Mag.*, vol. 43, no. 6, pp. 15–26, Dec. 2001.

[6] M. Nurnberger, "The broadband, shallow, reflecting cavity–backed slot spiral antenna," Ph.D. dissertation, University of Michigan, Ann arbor, Michigan, 2002.

[7] J. M. Bell and M. F. Iskander, "A Low–profile archimedean spiral antenna using an EBG ground plane," *IEEE Antennas and Wireless Propag. Lett.*, vol. 3, pp. 223–226, 2004.

[8] H. Nakano, S. Sasaki, H. Oyanagi, and J. Yamauchi, "Cavity-backed Archimedean spiral antenna with strip absorber," *IET Proc. Microw., Antennas Propag.*, vol. 2, no. 7, pp. 725–730, Oct. 2008.

[9] M. Radway and D. S. Filipovic, "Four-Armed Spiral-Helix Antenna," *IEEE Antennas and Wireless Propag. Lett.,* vol. 11, pp.338,341, 2012.

[10] M. W. Nurnberger and J. L. Volakis, "A new planar feed for slot spiral antennas," *IEEE Trans. Antennas, Propagat.*, vol. 44, pp. 130–131, Jan. 1996.

[11] R. Bawer and J. J. Wolfe, "The spiral antenna," *IRE Int. Convention Record*, pt. T., pp. 84–95, 1960.

[12] W. Sörgel and W. Wiesbeck, "Influence of the antennas on the ultrawideband transmission," *EURASIP J. Appl. Signal Process.*, no. 3, pp. 296–305, 2005.

[13] C. Roblin, "Representation, Characterization, and Modeling of Ultra Wide Band Antennas," in *Ultra Wide Band Antennas*. NJ: John Wiley, 2011, ch. 3.

[14] I. Oppermann, M. Hamalainen, and J. Iinatti*, UWB Theory and Applications*. New York: Wiley, 2004, ch. 3.